

Arbitrary Entropy Policy Optimization Breaks The Exploration Bottleneck of Reinforcement Learning

Chen Wang^{1,2} [†] Zhaochun Li^{2,3} [†] Jionghao Bai^{2,4} [†]
Yuzhi Zhang¹ ^{*} Shisheng Cui^{2,3} Zhou Zhao⁴ Yue Wang² ^{*}

Abstract

Reinforcement Learning (RL) is essential for enhancing the reasoning capabilities of large language models (LLMs), yet the widely adopted Group Relative Policy Optimization (GRPO) suffers from entropy collapse, causing exploration to vanish and policies to converge prematurely. As a result, RL is widely believed to be incapable of expanding the reasoning frontier of LLMs. Existing entropy-regularized methods introduce an inevitable trade-off between reward and entropy, leading to exploration accompanied by non-negligible optimization bias. In this work, we prove that temperature-guided REINFORCE can modulate policy entropy, and propose Arbitrary Entropy Policy Optimization (AEPO), which reformulates entropy regularization as a policy-gradient optimization problem. Rather than manipulating entropy directly, AEPO implicitly regulates it by applying a REINFORCE regularization term on temperature-adjusted samples, ensuring that entropy is controlled but never dominates optimization, thereby enabling arbitrary and principled entropy regulation. Experiments show that AEPO outperforms RL baselines on both pass@1 and pass@ k , and even surpasses the base model on pass@1024. By modulating entropy precisely, AEPO achieves more effective optimization dynamics and provides direct empirical evidence that entropy, exploration, and performance are intrinsically linked.

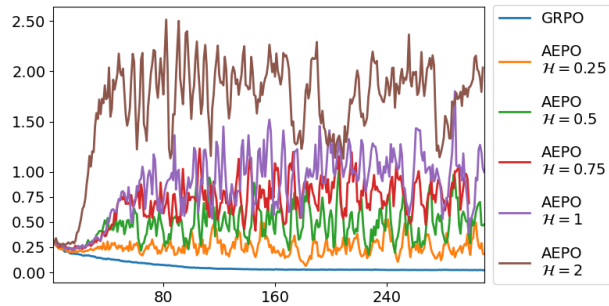


Figure 1: Entropy across five runs of AEPO. By adjusting only the parameter \mathcal{H} , entropy can be controlled at different levels.

1. Introduction

Reinforcement Learning (RL) has become a cornerstone for enhancing the reasoning capabilities of large language models (LLM) (GLM et al., 2024; Touvron et al., 2023; Schulman et al., 2017b; Rafailov et al., 2023; Zhong et al., 2024; Wang et al., 2024). Entropy reflects the extent of exploration by measuring the model’s uncertainty and output diversity during reasoning (Schulman et al., 2017a; Haarnoja et al., 2018; Nachum et al., 2017). Among existing approaches, Group Relative Policy Optimization (GRPO) has gained wide adoption due to its efficiency and scalability (Shao et al., 2024; Liu et al., 2024; Guo et al., 2025). However, GRPO suffers from a well-documented drawback: entropy collapse: As training progresses, policy entropy declines monotonically, sampled outputs converge to nearly identical solutions, and the model prematurely adopts a deterministic policy with limited exploration (Yu et al., 2025; Li et al., 2025; Zhang et al., 2025). This limits the ability of RL to discover diverse reasoning strategies. Recent studies have shown that RL fails to broaden the reasoning capabilities of LLMs; instead, it merely sharpens behaviors within the base model’s existing knowledge without introducing genuinely new reasoning patterns (Yue et al., 2025). This highlights the necessity of effective exploration in RL for LLMs, and such exploration fundamentally requires breaking the entropy bottleneck (Cui et al., 2025).

[†]Equal contribution, eamil: s-wc25@bjzgca.edu.cn. The code is available at <https://github.com/597358816/AEPO>

¹College of Software, Nankai University ²Zhongguancun Academy

³School of Automation, Beijing Institute of Technology ⁴College of Computer Science and Technology, Zhejiang University. *Correspondence to: Yuzhi Zhang <zyz@nankai.edu.cn>, Yue Wang <yuewang@bjzgca.edu.cn>.

Although the problem of entropy collapse in GRPO has been repeatedly recognized, it remains fundamentally unsolved. Most existing variants incorporate entropy as an additional reward term in the gradient, such as entropy regularization (Hou et al., 2025; Cui et al., 2025; Shen, 2025) or advantage-weighted bonuses (Cheng et al., 2025), to partially alleviate entropy collapse. However, these methods introduce an inevitable trade-off between reward and entropy, and thus bring non-negligible optimization bias when promoting exploration. In practice, entropy may oscillate between collapse and explosion instead of stabilizing in an optimal exploration regime, making the entropy-exploration-performance relationship hard to observe. As a result, it remains unclear whether entropy is a sufficient proxy for exploration and whether exploration itself consistently improves training outcomes. **If significant performance improvement can be observed by adjusting entropy to a better range, it would indicate that exploration plays a crucial role in this process. If arbitrary entropy control can be achieved during RL, it would make it possible to realize exploration at any desired degree and, in turn, establish a principled connection among entropy, exploration, and performance.**

Motivated by these challenges, we propose Arbitrary Entropy Policy Optimization (AEPO), which reformulates entropy regularization as a policy optimization, thereby fundamentally resolving entropy collapse. Instead of adding entropy bonuses, AEPO applies a REINFORCE policy gradient to temperature-adjusted samples, avoiding the unestimable bias introduced by conventional entropy-regularized methods. As shown in Fig. 1, AEPO maintains entropy oscillation around an arbitrary constant and is even theoretically capable of approximating arbitrary functions. AEPO achieves entropy control through three key design components:

- **Policy gradient as regularization:** Instead of using an entropy bonus, AEPO applies a full policy-gradient term to samples with naturally high or low entropy, preventing entropy from dominating optimization while enabling stable exploration.
- **Temperature as regularization:** Entropy is modulated through temperature-based sampling. When the current entropy falls below the target level, AEPO draws higher-temperature samples to increase entropy; when it exceeds the target, AEPO instead draws lower-temperature samples to reduce entropy.
- **REINFORCE as regularization:** In RLVR, the REINFORCE algorithm can filter out negative samples without introducing bias, allowing positive samples to form a unidirectional gradient toward a better distribution.

In summary, our contributions are threefold:

- **Breaking the entropy bottleneck:** We propose Arbitrary Entropy Policy Optimization, which can stabilize entropy at arbitrary target levels, effectively eliminating entropy collapse in GRPO and enabling exploration beyond the longstanding entropy bottleneck. AEPO introduces a REINFORCE regularization mechanism that controls entropy without distorting the optimization objective, representing a fundamentally new paradigm for exploration.
- **Breaking exploration bottleneck:** AEPO achieves consistent improvements over RL baselines on both pass@1 and pass@k, and even surpasses the base model on pass@1024, demonstrating that RL can conduct exploration rather than merely sharpening the base model’s knowledge.
- **Entropy–performance relation:** We find that merely adjusting entropy can directly influence training performance, providing explicit evidence for the correlation between entropy, exploration, and performance. Moreover, we observe a non-monotonic trend in which performance first increases and then decreases as entropy grows, highlighting the existence of an optimal entropy regime.

2. Related Work

RL has become a central paradigm for post-training large language models (LLMs), aligning them with human feedback and task-specific objectives. Early methods, such as RLHF, leveraged policy optimization (e.g., PPO) to encode human preferences (OpenAI, 2023; Team et al., 2024; Wei et al., 2023; Liu et al., 2023), while Direct Preference Optimization (DPO) (Rafailov et al., 2024) later improved efficiency by optimizing policies directly from preference data. Recent models like DeepSeek-R1 (Guo et al., 2025), and Kimi-1.5 (Team et al., 2025) extend RL through hybrid reward formulations and scalable optimization. Among them, Group Relative Policy Optimization (GRPO) (Shao et al., 2024; Liu et al., 2024) has become the de facto baseline for reasoning-focused RL, yet suffers from entropy collapse that limits exploration of diverse reasoning strategies.

Entropy has long been regarded as a proxy for exploration in reinforcement optimization. Classical methods employ entropy regularization to stabilize training and encourage diversity (Sutton et al., 1999; Williams, 1992). More recent studies extend this idea to GRPO by introducing entropy bonuses into rewards or advantages (Cheng et al., 2025; Cui et al., 2025; Shen, 2025). However, such approaches only yield coarse-grained effects: entropy still collapses as training proceeds, or the added bias distorts optimization.

In summary, existing methods lack a principled mechanism to precisely regulate entropy throughout training. Moreover, the role of entropy in driving exploration and its connection to downstream performance has not been quantitatively established. Our work addresses this gap by proposing Arbitrary Entropy Policy Optimization (AEPO), which enables controllable entropy regulation and provides explicit evidence of a non-monotonic relationship between entropy, exploration, and reasoning performance.

3. Preliminary

Our work focuses on fine-tuning LLM using Reinforcement Learning with Verifiable Reward (RLVR), such as mathematical reasoning and code generation.

Suppose the LLM is a softmax policy, that is

$$\pi_\theta(o_t|q_t) = \frac{\exp(l(q_t, o_t))}{\sum_{o'_t} \exp(l(q_t, o'_t))},$$

where q_t is the concatenation of query q followed by $o_{<t}$, and $l(q_t, o_t)$ is the logit of token o_t given input q_t . Furthermore, given a temperature T , we define:

$$\pi_\theta^T(o_t|q_t) = \frac{\exp(l(q_t, o_t)/T)}{\sum_{o'_t} \exp(l(q_t, o'_t)/T)}.$$

3.1. Policy-gradient based RL algorithms

Given a query q , let o denote a response sampled from policy π_θ for query q . Given a reward function:

$$R(q, o) = \mathbf{1}[o = o^*],$$

where o^* is the reference response for query q , the policy objective is:

$$\mathcal{J}(\theta) = \mathbb{E}_{q \sim P(Q), o \sim \pi_\theta(O|q)} \sum_{t=1}^{|o|} [R(q, o)].$$

To optimize the objective function, it is a common practice to use the Policy Gradient algorithm for gradient estimation:

$$\nabla_\theta \mathcal{J}_{REINFORCE}(\theta) = \mathbb{E}_{q \sim P(Q), o \sim \pi_\theta(O|q)} \sum_{t=1}^{|o|} [\nabla_\theta \log \pi_\theta(o_t|q, o_{<t}) \cdot R(q, o)],$$

$$\begin{aligned} \nabla_\theta \mathcal{J}_{GRPO}(\theta) &= \mathbb{E}_{q \sim P(Q), \{o_i\}_{i=1}^G \sim \pi_\theta(O|q)} \\ &\quad \frac{1}{G} \sum_{i=1}^G \frac{1}{|o_i|} \sum_{t=1}^{|o_i|} [\nabla_\theta \log \pi_\theta(o_t|q, o_{<t}) \cdot \hat{A}_{i,t}], \end{aligned}$$

where $R(q, o)$ is the reward for a query-response pair (q, o) , and $\hat{A}_{i,t}$ denotes the estimated advantage. To reduce gradient variance, GRPO extends REINFORCE by introducing

group-wise normalization: for each query q , it samples G responses $\{o_i\}_{i=1}^G$ and normalizes their rewards to compute the relative advantage for stable optimization.

$$\hat{A}_{i,t} = \frac{R(q, o_i) - \text{mean}(\{R(q, o_j)\}_{j=1}^G)}{\text{std}(\{R(q, o_j)\}_{j=1}^G)}.$$

3.2. Entropy-regularization variants

In traditional RL, it is common to add an entropy term to the objective to prevent the policy from becoming overly deterministic. Prior work has also explored various approaches in this direction for LLM training.

Entropy-Reg Given a query q , let o denote a response sampled from policy model π_θ for query q . For each token o_t in response o , we denote the token-level entropy as:

$$\mathcal{H}_t(\pi_\theta) := -\mathbb{E}_{o_t \sim \pi_\theta(\cdot|q, o_{<t})} [\log \pi_\theta(o_t|q, o_{<t})],$$

and then we can further denote that:

$$\mathcal{H}(\pi_\theta) := \mathbb{E}_{q \sim P(Q), o \sim \pi_\theta(O|q)} \frac{1}{|o|} \sum_{t=1}^{|o|} \mathcal{H}_t(\pi_\theta).$$

In maximum entropy RL, we optimize for the entropy-regularized objective as follows:

$$\begin{aligned} \mathcal{J}_{MaxEnt}(\theta) &= \mathcal{J}(\theta) + \lambda \cdot \mathcal{H}(\pi_\theta) = \\ &\quad \mathbb{E}_{q \sim P(Q), o \sim \pi_\theta(O|q)} \sum_{t=1}^{|o|} [R(q, o) - \lambda \cdot \log \pi_\theta(o_t|q, o_{<t})]. \end{aligned}$$

Entropy-Adv (Cheng et al., 2025) proposed an entropy-guided advantage shaping method. The key idea is to inject an entropy-based term into the advantage function during policy optimization. They define an entropy-based advantage term $\psi(\mathcal{H}_t)$ and use it to shape advantage:

$$\begin{aligned} \psi(\mathcal{H}_t) &= \min(\beta \cdot \mathcal{H}_t^{detach}, \frac{|\hat{A}_{i,t}|}{\kappa}), \\ A_{i,t}^{\text{shaped}} &= \hat{A}_{i,t} + \psi(\mathcal{H}_t), \end{aligned}$$

where $\beta > 0$ and $\kappa > 1$. The entropy term \mathcal{H}_t^{detach} is detached from the computational graph during backpropagation, acting as a fixed offset to the original advantage. The policy gradient of the algorithm retains a format similar to that in GRPO, where only the advantage $\hat{A}_{i,t}$ is replaced by the shaped one:

$$\begin{aligned} \nabla_\theta \mathcal{J}^{\text{shaped}}(\theta) &= \mathbb{E}_{q \sim P(Q), o \sim \pi_\theta(O|q)} \\ &\quad \sum_{t=1}^{|o|} [\nabla_\theta \log \pi_\theta(o_t|q, o_{<t}) \cdot A_{i,t}^{\text{shaped}}]. \end{aligned}$$

4. Method

Arbitrary Entropy Policy Optimization (AEPO) is designed to achieve precise and stable control of policy entropy during RL. This section first introduces the key theoretical premises underlying AEPO’s design, which reveal the relationship between temperature, entropy, and policy updates, and then details the algorithmic formulation of AEPO.

4.1. Theoretical analysis

The design of AEPO is built upon two empirical premises that connect temperature-based sampling to entropy dynamics. These analyses establish the foundation for controllable entropy modulation without introducing bias into the optimization objective.

Lemma 4.1. *Higher temperature distributions globally correspond to higher policy entropy, while lower temperature corresponds to lower entropy.*

Previous studies, such as [Du et al. \(2025\)](#), show that increasing the sampling temperature generally broadens the model’s output distribution and raises its entropy. In the context of RL, temperature can adjust entropy during inference, but it does not modify the underlying policy itself. Simply increasing temperature to force diverse outputs leads to off-policy sampling, which undermines the consistency required for policy optimization. What is needed instead is a mechanism that directly adjusts the policy itself so that the original policy is capable of generating more diverse behaviors.

Assumption 4.2. Assume that $T > 1$ and the actor policy π_θ is a tabular softmax policy updated via the following equation:

$$\theta_{k+1} = \theta_k + \eta \mathbb{E}_{a \sim \pi_{\theta_k}^T(\cdot|s)} [R(s, a) \cdot \nabla_\theta \log \pi_{\theta_k}(a|s)].$$

Theorem 4.3. Denote the function

$$\begin{aligned} \Delta H_k(T) &= -\eta \cdot \sum_{a^* \in \mathcal{A}^*} \pi_{\theta_k}^T(a^*|s) \times \\ &\quad \text{Cov}_{\pi_{\theta_k}}(z_k(s, a'), \delta_{a', a^*} - \pi_{\theta_k}(a'|s)). \end{aligned}$$

Then we have

$$\Delta H_k(T) \approx H(\theta_{k+1}) - H(\theta_k),$$

and

$$\Delta H'_k(T)|_{T=1} > 0 \quad \text{if} \quad \Delta H_k(T)|_{T=1} < 0.$$

The proof is provided in [Appendix B.5](#). In more intuitive terms, the preceding theorem implies that if the policy entropy begins to collapse during training, we can counteract this downward trend by performing updates using REINFORCE policy gradient of high-temperature samples.

Corollary 4.4. *High-temperature REINFORCE induces a relative increase in policy entropy, while low-temperature REINFORCE induces a relative decrease in policy entropy.*

Within the RLVR framework, the binary nature of the reward signal gives rise to an inherent filtering mechanism for negative samples. Building upon this property and the preceding premises, we can formulate a clear insight: computing the policy gradient with temperature-adjusted samples enables predictable and controllable entropy modulation. As illustrated in [Figure 2](#), entropy increases under high-temperature sampling and decreases under low-temperature sampling, with the increase typically occurring more gradually than the decrease. This dynamic forms the empirical foundation for AEPO’s temperature-controlled entropy feedback loop, allowing bidirectional regulation of entropy around a target value.

4.2. AEPO

Building on the theoretical premises described above, AEPO achieves stable and controllable entropy regulation by replacing explicit entropy bonuses with a REINFORCE-based regularization mechanism that adjusts the sampling temperature according to the current entropy state. Concretely, AEPO augments the GRPO objective (without KL divergence) with an additional policy gradient term applied to temperature-adjusted samples. The resulting policy gradient is given by:

$$\begin{aligned} &\nabla_\theta \mathcal{J}_{AEPO}(\theta) \\ &= \underbrace{\mathbb{E}_{q \sim P(Q), \{o_i\}_{i=1}^G \sim \pi_\theta(O|q)} \sum_{t=1}^{|o|} [\nabla_\theta \log \pi_\theta(o_t|q, o_{<t}) \cdot \hat{A}_{i,t}]}_{\text{GRPO form policy gradient}} \\ &\quad + \underbrace{\alpha \cdot \mathbb{E}_{q \sim P(Q), o \sim \pi_\theta^T(O|q)} \sum_{t=1}^{|o|} [\nabla_\theta \log \pi_\theta(o_t|q, o_{<t}) \cdot R(q, o)]}_{\text{REINFORCE form policy gradient}}. \end{aligned}$$

The implementation of AEPO’s loss function is shown in [Eq. \(1\)](#), which consists of three key design components:

Policy gradient as regularization. AEPO replaces conventional entropy regularization with a full policy gradient term that simultaneously enables entropy control and prevents entropy from dominating the optimization process. As illustrated in [Fig. 3](#), entropy regularization tends to drive the optimization toward two extremes—either entropy collapse or entropy explosion. In the former case, the regularization term is too weak to reverse the monotonic entropy decay; in the latter, entropy becomes an irreversible dominant factor in optimization. By contrast, AEPO constrains entropy

$$\begin{aligned}
\mathcal{J}_{GRPO}(\theta) &= \mathbb{E}_{q \sim P(Q), \{o_i\}_{i=1}^G \sim \pi_{\theta_{\text{old}}}(O|q)} \frac{1}{G} \sum_{i=1}^G \frac{1}{|o_i|} \sum_{t=1}^{|o_i|} \min \left[r_{i,t}(\theta) \hat{A}_{i,t}, \text{clip}(r_{i,t}(\theta), 1-\epsilon, 1+\epsilon) \hat{A}_{i,t} \right], \\
\mathcal{J}_{AEPO}(\theta) &= \mathcal{J}_{GRPO} + \alpha \mathbb{E}_{q \sim P(Q), \{o_i\}_{i=1}^G \sim \pi_{\theta_{\text{old}}}^T(O|q)} \frac{1}{|o_i|} \sum_{t=1}^{|o_i|} \min \left[r_{i,t}(\theta) R(q, o_i), \text{clip}(r_{i,t}(\theta), 1-\epsilon, 1+\epsilon) R(q, o_i) \right],
\end{aligned} \tag{1}$$

where $r_{i,t}(\theta) = \frac{\pi_\theta(o_{i,t}|q)}{\pi_{\theta_{\text{old}}}(o_{i,t}|q)}$ and $T = T_{\text{low}} + (T_{\text{high}} - T_{\text{low}}) \mathbf{1}[\mathcal{H}(\pi_{\theta_{\text{old}}}) < \mathcal{H}]$.

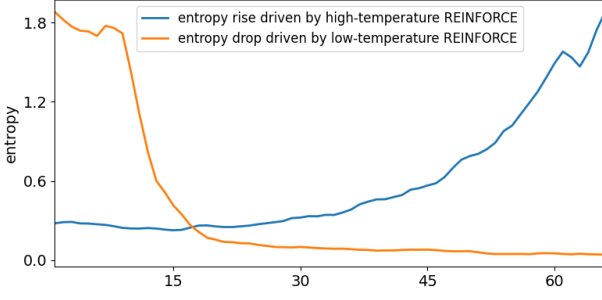


Figure 2: Entropy dynamics under temperature-controlled REINFORCE. High-temperature REINFORCE increases entropy, promoting exploration, while low-temperature REINFORCE reduces entropy.

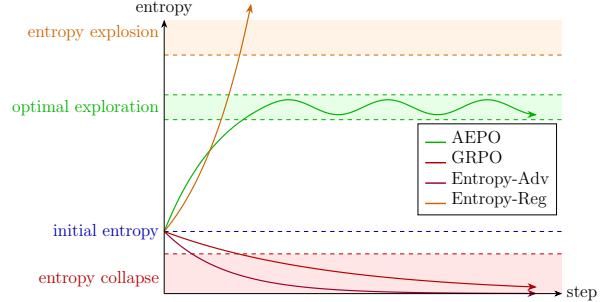


Figure 3: Comparison between entropy regularization and AEPO. Entropy regularization often drives optimization toward two extremes—collapse or explosion—while AEPO maintains entropy within a stable and optimal exploration range.

fluctuation within a narrow and stable range through the policy gradient mechanism, making it remarkably robust to hyperparameters.

Temperature as regularization. AEPO regulates the optimization direction by adjusting the sampling temperature. When the observed entropy $\mathcal{H}(\pi_{\theta_{\text{old}}})$ is below the target threshold \mathcal{H} , AEPO samples from the higher-temperature distribution $\pi_{\theta_{\text{old}}}^{T_{\text{high}}}$ to encourage exploration. Conversely, when $\mathcal{H}(\pi_{\theta_{\text{old}}})$ exceeds \mathcal{H} , AEPO samples from the lower-temperature distribution $\pi_{\theta_{\text{old}}}^{T_{\text{low}}}$ to promote stability. This bidirectional regulation mechanism achieves fine-grained entropy control, allowing the policy to maintain equilibrium between exploration and convergence.

REINFORCE as regularization. In RLVR, the reward space is binary. This property allows REINFORCE to filter out negative samples in an unbiased manner, ensuring that the gradient is formed from positive samples that align with the desired distribution. Consequently, AEPO’s regularization term produces an unidirectional optimization signal that guides the policy toward higher-quality behavior distributions.

5. Experiments

To validate the effectiveness of our methods, we present the experimental setup and results in the following sections. Our work is based on the EasyR1 and VeRL frameworks (YaoWei et al., 2025; Sheng et al., 2025), and we compare with the RL baselines GRPO (Shao et al., 2024) and its entropy-regularization variants (Hou et al., 2025; Cheng et al., 2025).

5.1. Experimental setup

Model and Dataset: We conduct experiments to evaluate the effectiveness of AEPO in RL for mathematical reasoning tasks. The base models include Qwen2.5-7B, Qwen2.5-Math-7B and Qwen3-4B. (Yang et al., 2024; 2025). For training, we use the DAPO-17K dataset (Yu et al., 2025), which contains diverse problem instances curated for RL.

Benchmark: Evaluation is performed on a broad suite of mathematical reasoning benchmarks, including AIME24, AIME25 (HuggingFaceH4, 2025), AMC (Lightman et al., 2023), GSM8K (Cobbe et al., 2021), MATH (Lightman et al., 2023), Minerva Math (Lewkowycz et al., 2022), and Olympiad (Lightman et al., 2023). These benchmarks col-

Table 1: AEPO demonstrates consistently superior performance across all mathematical reasoning benchmarks, surpassing GRPO, and all entropy-regularized baselines.

Benchmarks	AIME24 ₃₂	AIME25 ₃₂	AMC ₃₂	GSM8K	MATH	Minerva	Olympiad	Average
Qwen2.5-7B	7.91	5.31	36.2	88.5	64.4	22.0	29.3	36.24
+GRPO	17.1	7.60	65.8	92.3	75.6	36.8	38.8	47.70
+Entropy-Reg	13.6	8.85	67.4	92.3	76.8	35.5	39.1	47.65
+Entropy-Adv	14.8	8.23	67.3	91.9	76.6	38.2	37.5	47.79
+AEPO	17.5	11.4	69.3	92.9	78.0	37.8	40.2	49.57
Δ vs. GRPO	(+0.4)	(+3.8)	(+3.5)	(+0.6)	(+2.4)	(+1.0)	(+1.4)	(+1.87)
Qwen2.5-math-7B	15.5	7.81	42.1	65.4	59.4	11.0	26.7	32.56
+GRPO	32.1	11.0	72.4	88.7	80.6	34.6	41.8	51.60
+Entropy-Reg	31.4	10.1	74.3	87.0	78.8	35.7	40.4	51.10
+Entropy-Adv	32.1	11.4	72.1	87.8	78.8	37.5	42.1	51.76
+AEPO	36.4	12.6	74.8	89.5	82.6	38.2	43.0	53.87
Δ vs. GRPO	(+4.3)	(+1.6)	(+2.4)	(+0.8)	(+2.0)	(+3.6)	(+1.2)	(+2.27)
Qwen3-4B	36.4	22.7	71.9	93.9	84.8	42.3	47.2	57.03
+GRPO	52.9	41.5	86.1	95.2	92.0	46.7	60.0	67.77
+AEPO	54.5	43.7	89.7	95.0	92.8	47.8	60.9	69.20
Δ vs. GRPO	(+1.6)	(+2.2)	(+3.6)	(-0.2)	(+0.8)	(+1.1)	(+0.9)	(+1.43)

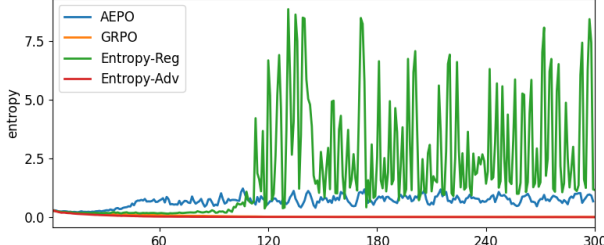


Figure 4: Entropy trajectories of AEPO compared with GRPO, Entropy-Reg, and Entropy-Adv. AEPO stabilizes entropy around a moderate level, demonstrating controllable and robust entropy regulation throughout training.

lectively span a wide range of difficulty levels, from grade school arithmetic to advanced competition-level mathematics, and together they cover nearly all mainstream benchmarks for mathematical reasoning, enabling a comprehensive assessment of AEPO’s impact on reasoning performance across diverse tasks.

5.2. Main results

Breaking the entropy bottleneck. Fig. 1 and 4 show that AEPO fundamentally resolves the entropy collapse issue that hampers GRPO and other RL baselines: AEPO maintains entropy around arbitrary target levels and avoids

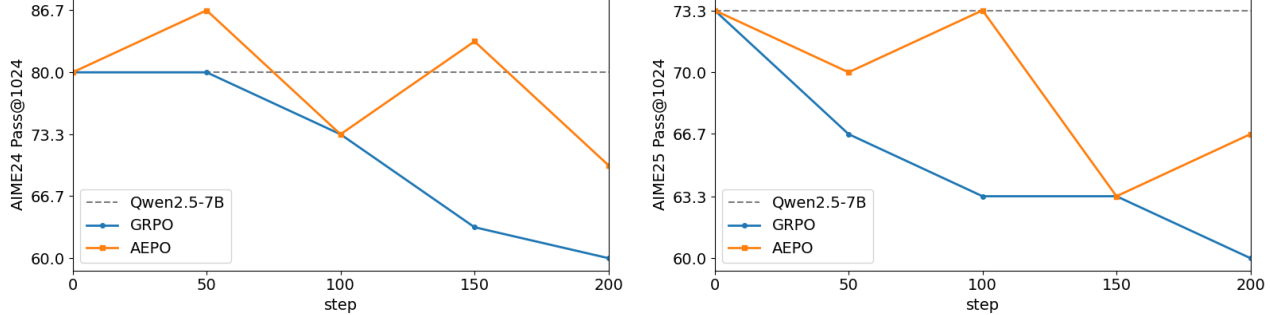
both collapse and uncontrolled expansion. As summarized in Table 1, on almost all mathematical reasoning benchmarks, AEPO surpasses GRPO and entropy-based baselines, demonstrating a much stronger capacity for effective exploration. In contrast, entropy-regularized baselines either fail to sustain entropy or introduce significant optimization bias that disrupts learning.

Breaking the exploration bottleneck. AEPO delivers consistent improvements over RL baselines on both pass@1 and pass@ k across every benchmark. More importantly, as shown in the Table. 2, AEPO shows the ability to explore broader than the base model on pass@1024, demonstrating that RL can meaningfully expand the reasoning frontier rather than merely sharpening the base model’s existing knowledge. During training, the pass@1024 performance of GRPO decreases monotonically, whereas AEPO shows the ability to expand the reasoning frontier, exhibiting upward trends rather than a purely decreasing curve. These results confirm that exploration can genuinely unlock new reasoning behaviors that are inaccessible to standard RL methods when guided by principled entropy modulation.

Entropy-performance relation. By varying the entropy target, AEPO enables a controlled study of how entropy affects exploration and downstream accuracy. Across all entropy levels, AEPO consistently outperforms GRPO, demonstrating that stable entropy regulation is inherently beneficial. More interestingly, as shown in Table 3, AEPO re-

Table 2: Comparison of pass@ k performance between the base model, GRPO, and AEPO across four mathematical reasoning benchmarks (steps ≥ 100). The accompanying figures show the evolution of pass@1024 of AEPO and GRPO on AIME24 and AIME25 during training.

Benchmarks	AIME24		AIME25		Minerva	Olympiad
	Pass@512	Pass@1024	Pass@512	Pass@1024	Pass@128	Pass@128
Qwen2.5-7B	71.7	80.0	61.7	73.3	69.8	77.8
+GRPO	63.3	73.3	60.0	63.3	65.8	72.9
+AEPO	70.0	83.3	66.7	73.3	67.0	74.1



veals a clear non-monotonic relationship: moderate entropy improves exploration and enhances performance, whereas overly high entropy disperses optimization and reduces accuracy. Different benchmarks also exhibit varying degrees of benefit from exploration; some continue to gain as entropy increases, while others experience performance degradation. Overall, the results display a rise-then-fall trend, indicating the presence of an optimal entropy regime for effective reasoning.

6. Ablation Study

To assess the contribution of each component in AEPO, we design two ablation studies to verify the necessity of temperature as regularization and REINFORCE as regularization for achieving effective entropy control.

6.1. Temperature as regularization

One critical component of AEPO is the use of temperature-adjusted samples for entropy control. In our design, the REINFORCE regularization term samples from a modified distribution, where the temperature T is adaptively adjusted based on the previous step’s entropy. This adjustment ensures that positive samples carry either higher or lower entropy as required, thereby stabilizing the overall entropy around the target threshold \mathcal{H} .

To validate the necessity of this design, we replace the temperature-adjusted distribution with the original distribution, as shown in Eq. (2) of Table 3. The results demonstrate

that when REINFORCE samples are drawn directly from the original policy distribution (i.e., without temperature adjustment), entropy control collapses: the policy entropy monotonically decreases during training, similar to GRPO. More importantly, the average benchmark score drops to 51.31, which is even worse than standard GRPO and far below AEPO (53.87). This shows that the variance of REINFORCE gradients, when unregularized by distribution adjustment, further degrades optimization performance.

These findings confirm that temperature adjustment is indispensable for AEPO: it directly enables controllable entropy regulation, and consistently improves reasoning performance across benchmarks. Moreover, it provides strong evidence for the relation between entropy and exploration: **the REINFORCE term in AEPO influences the exploration ability of the GRPO component through entropy control, thereby shaping the overall optimization dynamics during training.**

6.2. REINFORCE as regularization

Another essential component of AEPO is the use of REINFORCE gradients as a replacement for conventional entropy bonuses. In principle, REINFORCE allows unbiased estimation of gradients from positive samples while discarding negative ones, thereby forming a unidirectional optimization signal toward better distributions. This mechanism is critical for maintaining stable entropy control: when negative samples are included, the entropy-regularizing effect contributed by positive samples is counteracted, and the

Table 3: Ablation study on AEPO under different entropy targets, including benchmark performance across seven mathematical reasoning datasets. The upper table compares AEPO at various entropy levels, while the lower ablations illustrate how different loss formulations affect both performance and entropy stability.

Benchmarks	AIME24 ₃₂	AIME25 ₃₂	AMC ₃₂	GSM8K	MATH500	Minerva	Olympiad	Average
Qwen2.5-math-7B	15.5	7.81	42.1	65.4	59.4	11.0	26.7	37.66
+AEPO $\mathcal{H} = 0.25$	37.9	11.3	74.4	89.4	<u>79.8</u>	36.0	42.2	53.00
+AEPO $\mathcal{H} = 0.50$	<u>36.4</u>	12.6	<u>74.8</u>	89.5	82.6	38.2	43.0	53.87
+AEPO $\mathcal{H} = 0.75$	33.6	<u>15.1</u>	77.0	<u>89.4</u>	79.2	37.5	<u>42.4</u>	53.45
+AEPO $\mathcal{H} = 1.00$	33.2	15.6	74.8	88.7	79.6	<u>37.9</u>	42.1	53.13

Ablation loss and performance								Entropy control
$\mathcal{J}(\theta) = \mathcal{J}_{GRPO}(\theta) + \alpha \mathbb{E}_{q \sim P(Q), \{o_i\}_{i=1}^G \sim \pi_{\theta_{\text{old}}}(\mathcal{O} q)} \frac{1}{ O_i } \sum_{t=1}^{ O_i } \min \left[r_{i,t}(\theta) R(q, o_i), \text{clip}(r_{i,t}(\theta), 1 - \epsilon, 1 + \epsilon) R(q, o_i) \right] \quad (2)$								
AIME24	AIME25	AMC	GSM8K	MATH500	Minerva	Olympiad	Avg	Entropy collapse
31.4	11.8	74.5	88.9	79.0	33.5	40.1	51.31 (-2.56)	
$\mathcal{J}(\theta) = \mathcal{J}_{GRPO}(\theta) + \alpha \mathbb{E}_{q \sim P(Q), \{o_i\}_{i=1}^G \sim \pi_{\theta_{\text{old}}}^T(\mathcal{O} q)} \frac{1}{G} \sum_{i=1}^G \frac{1}{ O_i } \sum_{t=1}^{ O_i } \min \left[r_{i,t}(\theta) \hat{A}_{i,t}, \text{clip}(r_{i,t}(\theta), 1 - \epsilon, 1 + \epsilon) \hat{A}_{i,t} \right] \quad (3)$								
AIME24	AIME25	AMC	GSM8K	MATH500	Minerva	Olympiad	Avg	Entropy collapse
32.7	11.0	73.2	88.1	79.0	35.7	41.2	51.56 (-2.31)	

policy entropy eventually collapses.

To examine the role of REINFORCE, we conduct an ablation where the regularization term is still sampled from temperature-adjusted distributions, but the advantage function \hat{A}_t is used directly without filtering negative samples. As shown in Eq. (3) of Table 3, this variant fails to prevent entropy collapse, leading to degraded performance across benchmarks. The average score drops to 51.56. This confirms that filtering negative samples via REINFORCE is indispensable.

7. Conclusion and discussion

In this paper, we propose AEPO, a principled RL framework that addresses one of the most persistent challenges in RL—precise and stable entropy control. Unlike traditional entropy regularization methods that trade off exploration against stability, AEPO achieves controllable entropy regulation through a unified design that integrates policy gradient, distribution, and REINFORCE as regularization components. This formulation eliminates the entropy collapse phenomenon in GRPO and maintains policy entropy within an arbitrarily specified range, enabling balanced and consistent exploration throughout training.

Extensive experiments across seven mathematical reasoning benchmarks demonstrate that AEPO consistently outperforms entropy-based baselines on both pass@1 and pass@k,

exhibiting greater stability, generalization, and robustness to hyperparameters. Moreover, AEPO shows that RL-based exploration can indeed move beyond the limitations of the base model, confirming that reinforcement learning is capable of expanding the reasoning frontier rather than merely refining pretrained knowledge. More importantly, AEPO reveals a non-monotonic relationship between entropy and reasoning performance, showing that moderate entropy fosters exploration while excessive entropy impairs optimization—offering the first quantitative evidence linking entropy dynamics to reasoning capability in large language models.

Beyond entropy control, AEPO provides a broadly generalizable framework for learning under target distributions. The temperature-based mechanism used in AEPO should be viewed only as a special case: temperature creates the target distribution. When the task objective changes, the same principle naturally extends beyond entropy control. For example, if the goal is to mitigate overthinking by encouraging shorter responses, and if one can construct a transformed distribution π^* from the current policy π that produces more concise outputs while preserving correctness, then AEPO can use samples from π^* to form a REINFORCE regularization. In doing so, the current policy is gradually guided toward acquiring the desired properties of π^* . More generally, whenever a target distribution with specific behavioral characteristics can be derived from the current policy, AEPO draws samples from this target and applies a REINFORCE-based regularization term, enabling the current policy to

absorb the desired behavioral characteristics from the target distribution.

AEPO is not merely an entropy-control technique but a general paradigm for steering policies toward arbitrarily defined target behaviors through principled policy-gradient regularization. The same mechanism that adjusts the entropy can therefore be extended to new domains, illustrating the strong generalizability of AEPO.

Declaration of AI

AI is only used for translation and language polishing in this paper.

References

Cheng, D., Huang, S., Zhu, X., Dai, B., Zhao, W. X., Zhang, Z., and Wei, F. Reasoning with exploration: An entropy perspective. *arXiv preprint arXiv:2506.14758*, 2025.

Cobbe, K., Kosaraju, V., Bavarian, M., Chen, M., Jun, H., Kaiser, L., Plappert, M., Tworek, J., Hilton, J., Nakano, R., Hesse, C., and Schulman, J. Training verifiers to solve math word problems. *arXiv preprint arXiv:2110.14168*, 2021.

Cui, G., Zhang, Y., Chen, J., Yuan, L., Wang, Z., Zuo, Y., Li, H., Fan, Y., Chen, H., Chen, W., et al. The entropy mechanism of reinforcement learning for reasoning language models. *arXiv preprint arXiv:2505.22617*, 2025.

Du, W., Yang, Y., and Welleck, S. Optimizing temperature for language models with multi-sample inference. *arXiv preprint arXiv:2502.05234*, 2025.

GLM, T., Zeng, A., Xu, B., Wang, B., Zhang, C., Yin, D., Zhang, D., Rojas, D., Feng, G., Zhao, H., et al. Chatglm: A family of large language models from glm-130b to glm-4 all tools. *arXiv preprint arXiv:2406.12793*, 2024.

Guo, D., Yang, D., Zhang, H., Song, J., Zhang, R., Xu, R., Zhu, Q., Ma, S., Wang, P., Bi, X., et al. Deepseek-r1: Incentivizing reasoning capability in llms via reinforcement learning. *arXiv preprint arXiv:2501.12948*, 2025.

Haarnoja, T., Zhou, A., Abbeel, P., and Levine, S. Soft actor-critic: Off-policy maximum entropy deep reinforcement learning with a stochastic actor. In *International conference on machine learning*, pp. 1861–1870. Pmlr, 2018.

Hou, Z., Lv, X., Lu, R., Zhang, J., Li, Y., Yao, Z., Li, J., Tang, J., and Dong, Y. Advancing language model reasoning through reinforcement learning and inference scaling. *arXiv preprint arXiv:2501.11651*, 2025.

HuggingFaceH4. AIME 2024 Dataset (AIME I & II). https://huggingface.co/datasets/HuggingFaceH4/aime_2024, 2025.

Lewkowycz, A., Andreassen, A., Dohan, D., Dyer, E., Michalewski, H., Ramasesh, V., Sloane, A., Anil, C., Schlag, I., Gutman-Solo, T., et al. Solving quantitative reasoning problems with language models. *Advances in neural information processing systems*, 35:3843–3857, 2022.

Li, G., Lin, M., Galanti, T., Tu, Z., and Yang, T. Disco: Reinforcing large reasoning models with discriminative constrained optimization. *arXiv preprint arXiv:2505.12366*, 2025.

Lightman, H., Kosaraju, V., Burda, Y., Edwards, H., Baker, B., Lee, T., Leike, J., Schulman, J., Sutskever, I., and Cobbe, K. Let’s verify step by step. *arXiv preprint arXiv:2305.20050*, 2023.

Liu, A., Feng, B., Xue, B., Wang, B., Wu, B., Lu, C., Zhao, C., Deng, C., Zhang, C., Ruan, C., et al. Deepseek-v3 technical report. *arXiv preprint arXiv:2412.19437*, 2024.

Liu, H., Li, C., Wu, Q., and Lee, Y. J. Visual instruction tuning. *arXiv preprint arXiv:2304.08485*, 2023.

Nachum, O., Norouzi, M., Xu, K., and Schuurmans, D. Bridging the gap between value and policy based reinforcement learning. *Advances in neural information processing systems*, 30, 2017.

OpenAI. Gpt-4 technical report. *arXiv preprint arXiv:2303.08774*, 2023.

Rafailov, R., Sharma, A., Mitchell, E., Manning, C. D., Ermon, S., and Finn, C. Direct preference optimization: Your language model is secretly a reward model. *Advances in Neural Information Processing Systems*, 36: 53728–53741, 2023.

Rafailov, R., Sharma, A., Mitchell, E., Manning, C. D., Ermon, S., and Finn, C. Direct preference optimization: Your language model is secretly a reward model. *Advances in Neural Information Processing Systems*, 36, 2024.

Schulman, J., Chen, X., and Abbeel, P. Equivalence between policy gradients and soft q-learning. *arXiv preprint arXiv:1704.06440*, 2017a.

Schulman, J., Wolski, F., Dhariwal, P., Radford, A., and Klimov, O. Proximal policy optimization algorithms. *arXiv preprint arXiv:1707.06347*, 2017b.

Shao, Z., Wang, P., Zhu, Q., Xu, R., Song, J., Bi, X., Zhang, H., Zhang, M., Li, Y., Wu, Y., et al. Deepseekmath: Pushing the limits of mathematical reasoning in open language models. *arXiv preprint arXiv:2402.03300*, 2024.

Shen, H. On entropy control in llm-rl algorithms. *arXiv preprint arXiv:2509.03493*, 2025.

Sheng, G., Zhang, C., Ye, Z., Wu, X., Zhang, W., Zhang, R., Peng, Y., Lin, H., and Wu, C. Hybridflow: A flexible and efficient rlhf framework. In *Proceedings of the Twentieth European Conference on Computer Systems*, pp. 1279–1297, 2025.

Sutton, R. S., McAllester, D., Singh, S., and Mansour, Y. Policy gradient methods for reinforcement learning with function approximation. *Advances in neural information processing systems*, 12, 1999.

Team, G., Georgiev, P., Lei, V. I., Burnell, R., Bai, L., Gulati, A., Tanzer, G., Vincent, D., Pan, Z., Wang, S., et al. Gemini 1.5: Unlocking multimodal understanding across millions of tokens of context. *arXiv preprint arXiv:2403.05530*, 2024.

Team, K., Du, A., Gao, B., Xing, B., Jiang, C., Chen, C., Li, C., Xiao, C., Du, C., Liao, C., et al. Kimi k1. 5: Scaling reinforcement learning with llms. *arXiv preprint arXiv:2501.12599*, 2025.

Touvron, H., Martin, L., Stone, K., Albert, P., Almahairi, A., Babaei, Y., Bashlykov, N., Batra, S., Bhargava, P., Bhosale, S., et al. Llama 2: Open foundation and fine-tuned chat models. *arXiv preprint arXiv:2307.09288*, 2023.

Wang, Z., Bi, B., Pentyala, S. K., Ramnath, K., Chaudhuri, S., Mehrotra, S., Mao, X.-B., Asur, S., et al. A comprehensive survey of llm alignment techniques: Rlhf, rlaif, ppo, dpo and more. *arXiv preprint arXiv:2407.16216*, 2024.

Wei, L., Jiang, Z., Huang, W., and Sun, L. Instructiongpt-4: A 200-instruction paradigm for fine-tuning minigpt-4. *arXiv preprint arXiv:2308.12067*, 2023.

Williams, R. J. Simple statistical gradient-following algorithms for connectionist reinforcement learning. *Machine learning*, 8(3):229–256, 1992.

Yang, A., Yang, B., Zhang, B., Hui, B., Zheng, B., Yu, B., Li, C., Liu, D., Huang, F., Wei, H., et al. Qwen2. 5 technical report. *arXiv preprint arXiv:2412.15115*, 2024.

Yang, A., Li, A., Yang, B., Zhang, B., Hui, B., Zheng, B., Yu, B., Gao, C., Huang, C., Lv, C., et al. Qwen3 technical report. *arXiv preprint arXiv:2505.09388*, 2025.

Yaowei, Z., Junting, L., Shenzhi, W., Zhangchi, F., Dong-dong, K., and Yuwen, X. Easyr1: An efficient, scalable, multi-modality rl training framework. <https://github.com/hiyouga/EasyR1>, 2025.

Yu, Q., Zhang, Z., Zhu, R., Yuan, Y., Zuo, X., Yue, Y., Fan, T., Liu, G., Liu, L., Liu, X., et al. Dapo: An open-source llm reinforcement learning system at scale. *arXiv preprint arXiv:2503.14476*, 2025.

Yue, Y., Chen, Z., Lu, R., Zhao, A., Wang, Z., Song, S., and Huang, G. Does reinforcement learning really incentivize reasoning capacity in llms beyond the base model? *arXiv preprint arXiv:2504.13837*, 2025.

Zhang, X., Wen, S., Wu, W., and Huang, L. Edge-grpo: Entropy-driven grpo with guided error correction for advantage diversity. *arXiv preprint arXiv:2507.21848*, 2025.

Zhong, H., Shan, Z., Feng, G., Xiong, W., Cheng, X., Zhao, L., He, D., Bian, J., and Wang, L. Dpo meets ppo: Reinforced token optimization for rlhf. *arXiv preprint arXiv:2404.18922*, 2024.

A. Detailed implementation:

We follow the default EasyR1 setup for all experiments and run all models on 8 A800 GPUs. The full training configuration is listed in Table 4.

Table 4: Detailed implementation for all experiments.

Hardware	8 × A800 GPUs (40GB)
RL Settings:	
Maximum response length	
Batch size	8192
Mini batch size	512
Rollout group size G	128
Sampling temperature	8
Learning rate	1.0
Clip range $\epsilon = \epsilon_{low} = \epsilon_{high}$	1×10^{-6}
Reward type	0.2
Binary reward	
AEPO Settings:	
High temperature T_{high}	0.2
Low temperature T_{low}	0.8
Temperature-adjusted REINFORCE samples	60 (positive samples per step) for entropy up 30 for entropy down
Entropy-Regularized Baselines:	
Entropy-Reg coefficient λ	0.015
Entropy-Adv parameters (β, κ)	(0.4, 2)
Evaluation Settings:	
Maximum response length	8192
Top P	0.95
Temperature	0.1 for Pass@1 1.0 for Pass@k

B. Proof of Theorem 4.3

Reinforcement Learning. Let o denote a response sampled from the policy $\pi_\theta(\cdot|s_0)$ for query s_0 . Given a reward function $R(s_0, o) \in \mathbb{R}$, the policy objective is

$$J(\theta) = \mathbb{E}_{s_0 \sim \rho} \mathbb{E}_{o \sim \pi_\theta(O|s_0)} [R(o)]$$

$$\nabla_\theta J(\theta) = \mathbb{E}_{s_0 \sim \rho} \mathbb{E}_{o \sim \pi_\theta(O|s_0)} [R(o) \cdot \sum_{t=0}^{T-1} \nabla_\theta \log \pi_\theta(o_t|s_t)]$$

Definition B.1. policy entropy: $H(\theta) = -\mathbb{E}_{s_0 \sim \rho} \mathbb{E}_{o \sim \pi_\theta(O|s_0)} [\frac{1}{|o|} \sum_{t=0}^{|o|-1} \mathbb{E}_{o_t \sim \pi_\theta(\cdot|s_t)} [\log \pi_\theta(o_t|s_t)]]$

To simplify the analysis, let us consider the particular case in which $|o| = 1$. For a given initial state s , a corresponding action space \mathcal{A} , and a given reward function

$$R(s, a) = \begin{cases} 1 & \text{if } a \in \mathcal{A}^* \\ 0 & \text{otherwise} \end{cases}$$

where \mathcal{A}^* denotes the set of reference actions for a given state s , we have some simplified definitions as follows:

Definition B.2. simplified objective: $J(\theta) = \mathbb{E}_{a \sim \pi_\theta(\cdot|s)}[R(s, a)]$

Definition B.3. simplified policy entropy: $H(\theta) = -\mathbb{E}_{a \sim \pi_\theta(\cdot|s)}[\log \pi_\theta(a|s)]$

We first consider an intrinsic property of LLMs: they are softmax policies, which means the policies are parameterized by

$$\pi_\theta(a|s) = \frac{\exp(z(s, a))}{\sum_{a' \in \mathcal{A}} \exp(z(s, a'))}$$

where $z(s, a)$ is the logit for the state-action pair (s, a) under parameter θ . Furthermore, given a temperature T , we define:

$$\pi_\theta^T(a|s) = \frac{\exp(\frac{z(s, a)}{T})}{\sum_{a' \in \mathcal{A}} \exp(\frac{z(s, a')}{T})}$$

we write $z_{\theta_k}(s, a)$ simply as $z_k(s, a)$, and we write $\pi_\theta^T(a|s)$ simply as $\pi_\theta(a|s)$ when $T = 1$.

Problem 1. To optimize the RL objective above, we usually apply the gradient ascent method. We can calculate the policy gradient as

$$\nabla_\theta J(\theta) = \mathbb{E}_{a \sim \pi_\theta(\cdot|s)}[R(s, a) \cdot \nabla_\theta \log \pi_\theta(a|s)],$$

And then we can update the parameter according to the following rule:

$$\theta_{k+1} = \theta_k + \eta \cdot \nabla_\theta J(\theta_k) = \theta_k + \eta \cdot \mathbb{E}_{a \sim \pi_{\theta_k}(\cdot|s)}[R(s, a) \cdot \nabla_\theta \log \pi_{\theta_k}(a|s)].$$

Empirically, we observe that applying the aforementioned update rule leads to a decreasing trend in policy entropy. This leads to the natural question: How is this trend affected if we modify the sampling distribution for policy gradient estimation?

We consider a more general parameter update rule based on the standard gradient ascent rule.

$$\theta_{k+1} = \theta_k + \eta \cdot \mathbb{E}_{a \sim \pi_{\theta_k}^T(\cdot|s)}[R(s, a) \cdot \nabla_\theta \log \pi_{\theta_k}(a|s)] \quad (4)$$

When we set the temperature $T = 1$, the update rule above becomes identical to the standard gradient ascent method. In the following, we will investigate how the policy entropy changes with the parameter update defined as Eq.4

Assumption B.4. $\langle \nabla_\theta z_k(s, a), \nabla_\theta z_k(s, b) \rangle = c_{a,b} \cdot \delta_{a,b}$, $\forall a, b \in \mathcal{A}$. where $c_{a,b} \in \mathbb{R}$ and $\delta_{a,b} = \mathbf{1}[a = b]$. In the following, we set $c_{a,b} \equiv 1$.

Lemma B.5. Let the sequence of parameters $\{\theta_k\}$ be governed by the update rule described above. Denote the function

$$\Delta H_k(T) = -\eta \cdot \sum_{a^* \in \mathcal{A}^*} \pi_{\theta_k}^T(a^*|s) \cdot \text{Cov}_{\pi_{\theta_k}}(z_k(s, a'), \delta_{a', a^*} - \pi_{\theta_k}(a'|s)).$$

Then we have

$$\Delta H_k(T) \approx H(\theta_{k+1}) - H(\theta_k),$$

and

$$\Delta H_k'(T)|_{T=1} > 0 \quad \text{if} \quad \Delta H_k(T)|_{T=1} < 0.$$

Proof. For a given parameter θ_k and a relatively small learning rate η , leveraging Taylor's expansion under first-order approximation, we have

$$H(\theta_{k+1}) - H(\theta_k) \approx \langle \nabla_\theta H(\theta_k), \theta_{k+1} - \theta_k \rangle$$

We then to derive what $\nabla_\theta H(\theta_k)$ is, according to the definition of H , we have

$$\begin{aligned} \nabla_\theta H(\theta_k) &= -\nabla_\theta \mathbb{E}_{a \sim \pi_{\theta_k}(\cdot|s)}[\log \pi_{\theta_k}(a|s)] \\ &= -\nabla_\theta \sum_{a \in \mathcal{A}} [\pi_{\theta_k}(a|s) \cdot \log \pi_{\theta_k}(a|s)] \\ &= -\mathbb{E}_{a \sim \pi_{\theta_k}} [\nabla_\theta \log \pi_{\theta_k}(a|s) \cdot \log \pi_{\theta_k}(a|s) + \nabla_\theta \log \pi_{\theta_k}(a|s)] \\ &= -\mathbb{E}_{a \sim \pi_{\theta_k}} [\nabla_\theta \log \pi_{\theta_k}(a|s) \cdot \log \pi_{\theta_k}(a|s)] \end{aligned}$$

the last equality follows from $\sum_{a \in \mathcal{A}} \nabla_{\theta} \pi_{\theta_k}(a|s) = \nabla_{\theta} \sum_{a \in \mathcal{A}} \pi_{\theta_k}(a|s) = \nabla_{\theta} 1 = 0$.

Then we have

$$\begin{aligned} H(\theta_{k+1}) - H(\theta_k) &\approx - \langle \mathbb{E}_{a \sim \pi_{\theta_k}(\cdot|s)} [\nabla_{\theta} \log \pi_{\theta_k}(a|s) \cdot \log \pi_{\theta_k}(a|s)], \theta_{k+1} - \theta_k \rangle \\ &= -\mathbb{E}_{a \sim \pi_{\theta_k}(\cdot|s)} [\log \pi_{\theta_k}(a|s) \cdot \langle \nabla_{\theta} \log \pi_{\theta_k}(a|s), \theta_{k+1} - \theta_k \rangle] \\ &\approx -\mathbb{E}_{a \sim \pi_{\theta_k}(\cdot|s)} [\log \pi_{\theta_k}(a|s) \cdot (\log \pi_{\theta_{k+1}}(a|s) - \log \pi_{\theta_k}(a|s))] \\ &\approx -\mathbb{E}_{a \sim \pi_{\theta_k}(\cdot|s)} [\log \pi_{\theta_k}(a|s) \cdot \sum_{a' \in \mathcal{A}} \frac{\mathbf{d} \log \pi_{\theta_k}(a|s)}{\mathbf{d} z_k(s, a')} \cdot \Delta z_k(s, a')] \end{aligned}$$

We now evaluate the two terms, $\frac{\mathbf{d} \log \pi_{\theta_k}(a|s)}{\mathbf{d} z_k(s, a')}$ and $\Delta z_k(s, a')$, in turn.

$$\begin{aligned} \frac{\mathbf{d} \log \pi_{\theta_k}(a|s)}{\mathbf{d} z_k(s, a')} &= \delta_{a, a'} - \pi_{\theta_k}(a'|s); \\ \Delta z_k(s, a') &\approx \langle \frac{\mathbf{d} z_k(s, a')}{\mathbf{d} \theta}, \theta_{k+1} - \theta_k \rangle \\ &= \langle \nabla_{\theta} z_k(s, a'), \eta \cdot \mathbb{E}_{a \sim \pi_{\theta_k}^T(\cdot|s)} [R(s, a) \cdot \nabla_{\theta} \log \pi_{\theta_k}(a|s)] \rangle \\ &= \eta \cdot \sum_{a^* \in \mathcal{A}^*} \pi_{\theta_k}^T(a^*|s) \cdot \langle \nabla_{\theta} z_k(s, a'), \nabla_{\theta} z_k(s, a^*) - \mathbb{E}_{a \sim \pi_{\theta_k}} [\nabla_{\theta} z_k(s, a)] \rangle \\ &= \eta \cdot \sum_{a^* \in \mathcal{A}^*} [\pi_{\theta_k}^T(a^*|s) \cdot (\delta_{a', a^*} - \pi_{\theta_k}(a'|s))] \end{aligned} \tag{5}$$

where the first equality in Eq.5 follows from

$$\begin{aligned} \nabla_{\theta} \log \pi_{\theta_k}(a|s) &= \nabla_{\theta} [z_k(s, a) - \log \sum_{a' \in \mathcal{A}} \exp(z_k(s, a'))] \\ &= \nabla_{\theta} z_k(s, a) - \frac{1}{\sum_{a' \in \mathcal{A}} \exp(z_k(s, a'))} \left(\sum_{a' \in \mathcal{A}} \exp(z_k(s, a')) \cdot \nabla_{\theta} z_k(s, a') \right) \\ &= \nabla_{\theta} z_k(s, a) - \mathbb{E}_{a \sim \pi_{\theta_k}} [\nabla_{\theta} z_k(s, a)] \end{aligned}$$

and the last equality in Eq.5 follows from assumption 1. Then, we have

$$\begin{aligned} H(\theta_{k+1}) - H(\theta_k) &\approx - \sum_{a' \in \mathcal{A}} \Delta z_k(s, a') \cdot \mathbb{E}_{a \sim \pi_{\theta_k}(\cdot|s)} [\log \pi_{\theta_k}(a|s) \cdot \frac{\mathbf{d} \log \pi_{\theta_k}(a|s)}{\mathbf{d} z_k(s, a')}] \\ &= - \sum_{a' \in \mathcal{A}} \Delta z_k(s, a') \cdot \mathbb{E}_{a \sim \pi_{\theta_k}(\cdot|s)} [\log \pi_{\theta_k}(a|s) \cdot (\delta_{a, a'} - \pi_{\theta_k}(a'|s))] \\ &= - \sum_{a' \in \mathcal{A}} \Delta z_k(s, a') \cdot [\pi_{\theta_k}(a'|s) \cdot \log \pi_{\theta_k}(a'|s) - \pi_{\theta_k}(a'|s) \cdot \mathbb{E}_{a \sim \pi_{\theta_k}(\cdot|s)} [\log \pi_{\theta_k}(a|s)]] \\ &= - (\mathbb{E}_{a \sim \pi_{\theta_k}(\cdot|s)} [\Delta z_k(s, a) \cdot \log \pi_{\theta_k}(a|s)] - \mathbb{E}_{a \sim \pi_{\theta_k}(\cdot|s)} [\Delta z_k(s, a)] \cdot \mathbb{E}_{a \sim \pi_{\theta_k}(\cdot|s)} [\log \pi_{\theta_k}(a|s)]) \\ &= - \text{Cov}_{\pi_{\theta_k}} (\Delta z_k(s, a), \log \pi_{\theta_k}(a|s)) \\ &= - \text{Cov}_{\pi_{\theta_k}} (\Delta z_k(s, a), z_k(a|s)), \end{aligned} \tag{6}$$

take Eq.5 into Eq.6, we have

$$H(\theta_{k+1}) - H(\theta_k) \approx -\eta \cdot \sum_{a^* \in \mathcal{A}^*} \pi_{\theta_k}^T(a^*|s) \cdot \text{Cov}_{\pi_{\theta_k}} (z_k(s, a), \delta_{a, a^*} - \pi_{\theta_k}(a|s)) \equiv \Delta H_k(T)$$

We now proceed to the proof of the second part of the lemma. We first partition the set \mathcal{A}^* into three subsets: \mathcal{A}_1 , \mathcal{A}_2 , and \mathcal{A}_3 , where

$$\begin{aligned} \mathcal{A}_1 &= \{a | a \in \mathcal{A}^*, z_k(s, a) < \mathbb{E}_{a' \sim \pi_{\theta_k}(\cdot|s)} [z(s, a')]\}; \\ \mathcal{A}_2 &= \{a | a \in \mathcal{A}^*, z_k(s, a) \geq \mathbb{E}_{a' \sim \pi_{\theta_k}(\cdot|s)} [z(s, a')], \text{Cov}_{a' \sim \pi_{\theta_k}} (z_k(s, a'), \delta_{a', a}) < C_{\pi_k}\}; \\ \mathcal{A}_3 &= \{a | a \in \mathcal{A}^*, z_k(s, a) \geq \mathbb{E}_{a' \sim \pi_{\theta_k}(\cdot|s)} [z(s, a')], \text{Cov}_{a' \sim \pi_{\theta_k}} (z_k(s, a'), \delta_{a', a}) \geq C_{\pi_k}\} \end{aligned}$$

where $C_{\pi_k} = \text{Cov}_{a' \sim \pi_{\theta_k}}(z_k(s, a'), \pi_{\theta_k}(a'|s))$. According to the condition, we have

$$\begin{aligned} 0 &\leq \sum_{a^* \in \mathcal{A}^*} \pi_{\theta_k}(a^*|s) \cdot \text{Cov}_{\pi_{\theta_k}}(z_k(s, a), \delta_{a, a^*} - \pi_{\theta_k}(a|s)) \\ &= \sum_{i=1}^3 \sum_{a^* \in \mathcal{A}_i} \pi_{\theta_k}(a^*|s) \cdot \text{Cov}_{\pi_{\theta_k}}(z_k(s, a), \delta_{a, a^*} - \pi_{\theta_k}(a|s)) \\ &\leq \sum_{a^* \in \mathcal{A}_2 \cup \mathcal{A}_3} \pi_{\theta_k}(a^*|s) \cdot \text{Cov}_{\pi_{\theta_k}}(z_k(s, a), \delta_{a, a^*} - \pi_{\theta_k}(a|s)) \end{aligned}$$

We now turn to the analysis of $\frac{\mathbf{d}\Delta H_k(T)}{\mathbf{d}T}$.

$$\begin{aligned} \frac{\mathbf{d}\pi_{\theta_k}^T(a|s)}{\mathbf{d}T} &= \frac{1}{(\sum_{a' \in \mathcal{A}} \exp(\frac{z_k(s, a')}{T}))^2} \cdot [\exp(\frac{z_k(s, a)}{T})(-T^{-2})z_k(s, a) \sum_{a' \in \mathcal{A}} \exp(\frac{z_k(s, a')}{T}) \\ &\quad - \exp(\frac{z_k(s, a)}{T}) \sum_{a' \in \mathcal{A}} (-T^{-2})\exp(\frac{z_k(s, a')}{T})z_k(s, a')] \\ &= -T^{-2} \cdot \pi_{\theta_k}^T(a|s) \cdot [z_k(s, a) - \mathbb{E}_{\pi_{\theta_k}^T}[z_k(s, a')]] \end{aligned}$$

when we take $T = 1$, we have

$$\frac{\mathbf{d}\pi_{\theta_k}^T(a|s)}{\mathbf{d}T}|_{T=1} = -\pi_{\theta_k}(a|s) \cdot [z_k(s, a) - \mathbb{E}_{\pi_{\theta_k}}[z_k(s, a')]] = -\text{Cov}_{\pi_{\theta_k}}(z_k(s, a'), \delta_{a, a'})$$

$$\begin{aligned} \frac{\mathbf{d}\Delta H(T)}{\mathbf{d}T}|_{T=1} &= -\eta \cdot \sum_{a^* \in \mathcal{A}^*} \text{Cov}_{\pi_{\theta_k}}(z_k(s, a'), \delta_{a', a^*} - \pi_{\theta_k}(a'|s)) \cdot \frac{\mathbf{d}\pi_{\theta_k}^T(a^*|s)}{\mathbf{d}T} \\ &= -\eta \cdot \sum_{a^* \in \mathcal{A}^*} \text{Cov}_{\pi_{\theta_k}}(z_k(s, a'), \delta_{a', a^*} - \pi_{\theta_k}(a'|s)) \cdot (-\text{Cov}_{\pi_{\theta_k}}(z_k(s, a'), \delta_{a', a^*})) \\ &= \eta \cdot \sum_{a^* \in \mathcal{A}_1 \cup \mathcal{A}_2 \cup \mathcal{A}_3} \text{Cov}_{\pi_{\theta_k}}(z_k(s, a'), \delta_{a', a^*} - \pi_{\theta_k}(a'|s)) \cdot \text{Cov}_{\pi_{\theta_k}}(z_k(s, a'), \delta_{a', a^*}) \end{aligned}$$

We now proceed with a case-by-case analysis based on different a^* . For $a^* \in \mathcal{A}_1$, we have $z_k(s, a) < \mathbb{E}_{a' \sim \pi_{\theta_k}(\cdot|s)}[z(s, a')]$, and then we can get $\text{Cov}_{\pi_{\theta_k}}(z_k(s, a'), \delta_{a', a^*}) < 0$, also we have $\text{Cov}_{\pi_{\theta_k}}(z_k(s, a'), \delta_{a', a^*} - \pi_{\theta_k}(a'|s)) < 0$, therefore

$$\sum_{a^* \in \mathcal{A}_1} \text{Cov}_{\pi_{\theta_k}}(z_k(s, a'), \delta_{a', a^*} - \pi_{\theta_k}(a'|s)) \cdot \text{Cov}_{\pi_{\theta_k}}(z_k(s, a'), \delta_{a', a^*}) \geq 0,$$

For $a^* \in \mathcal{A}_2$, we have $z_k(s, a^*) \geq \mathbb{E}_{a' \sim \pi_{\theta_k}(\cdot|s)}[z(s, a')]$ and $\text{Cov}_{a' \sim \pi_{\theta_k}}(z_k(s, a'), \delta_{a', a^*}) < C_{\pi_k}$, we set $u = \max_{a^* \in \mathcal{A}_2} \{z_k(s, a^*)\}$, therefore

$$\begin{aligned} &\sum_{a^* \in \mathcal{A}_2} \text{Cov}_{\pi_{\theta_k}}(z_k(s, a'), \delta_{a', a^*} - \pi_{\theta_k}(a'|s)) \cdot \text{Cov}_{\pi_{\theta_k}}(z_k(s, a'), \delta_{a', a^*}) \\ &= \sum_{a^* \in \mathcal{A}_2} \text{Cov}_{\pi_{\theta_k}}(z_k(s, a'), \delta_{a', a^*} - \pi_{\theta_k}(a'|s)) \cdot \pi_{\theta_k}(a^*|s) \cdot [z_k(s, a^*) - \mathbb{E}_{\pi_{\theta_k}}[z_k(s, a')]] \\ &= \sum_{a^* \in \mathcal{A}_2} \underbrace{\text{Cov}_{\pi_{\theta_k}}(z_k(s, a'), \delta_{a', a^*} - \pi_{\theta_k}(a'|s))}_{< 0} \cdot \pi_{\theta_k}(a^*|s) \cdot \underbrace{[z_k(s, a^*) - u + u - \mathbb{E}_{\pi_{\theta_k}}[z_k(s, a')]]}_{\leq 0} \\ &\geq \sum_{a^* \in \mathcal{A}_2} \text{Cov}_{\pi_{\theta_k}}(z_k(s, a'), \delta_{a', a^*} - \pi_{\theta_k}(a'|s)) \cdot \pi_{\theta_k}(a^*|s) \cdot [u - \mathbb{E}_{\pi_{\theta_k}}[z_k(s, a')]], \end{aligned}$$

For $a^* \in \mathcal{A}_3$, we have

$$\begin{aligned}
& \sum_{a^* \in \mathcal{A}_3} \text{Cov}_{\pi_{\theta_k}}(z_k(s, a'), \delta_{a', a^*} - \pi_{\theta_k}(a'|s)) \cdot \text{Cov}_{\pi_{\theta_k}}(z_k(s, a'), \delta_{a', a^*}) \\
&= \sum_{a^* \in \mathcal{A}_3} \text{Cov}_{\pi_{\theta_k}}(z_k(s, a'), \delta_{a', a^*} - \pi_{\theta_k}(a'|s)) \cdot \pi_{\theta_k}(a^*|s) \cdot [z_k(s, a^*) - \mathbb{E}_{\pi_{\theta_k}}[z_k(s, a')]] \\
&= \sum_{a^* \in \mathcal{A}_3} \underbrace{\text{Cov}_{\pi_{\theta_k}}(z_k(s, a'), \delta_{a', a^*} - \pi_{\theta_k}(a'|s)) \cdot \pi_{\theta_k}(a^*|s)}_{>0} \cdot \underbrace{[z_k(s, a^*) - u + u - \mathbb{E}_{\pi_{\theta_k}}[z_k(s, a')]]}_{\geq 0} \\
&\geq \sum_{a^* \in \mathcal{A}_3} \text{Cov}_{\pi_{\theta_k}}(z_k(s, a'), \delta_{a', a^*} - \pi_{\theta_k}(a'|s)) \cdot \pi_{\theta_k}(a^*|s) \cdot [u - \mathbb{E}_{\pi_{\theta_k}}[z_k(s, a')]],
\end{aligned}$$

Therefore, combining the results from the three cases discussed above, we arrive at the following conclusion:

$$\begin{aligned}
& \frac{d\Delta H(T)}{dT} \Big|_{T=1} \\
&= \eta \cdot \left[\sum_{a^* \in \mathcal{A}_1 \cup \mathcal{A}_2 \cup \mathcal{A}_3} \text{Cov}_{\pi_{\theta_k}}(z_k(s, a'), \delta_{a', a^*} - \pi_{\theta_k}(a'|s)) \cdot \text{Cov}_{\pi_{\theta_k}}(z_k(s, a'), \delta_{a', a^*}) \right] \\
&\geq \eta \cdot \left[\sum_{a^* \in \mathcal{A}_2 \cup \mathcal{A}_3} \text{Cov}_{\pi_{\theta_k}}(z_k(s, a'), \delta_{a', a^*} - \pi_{\theta_k}(a'|s)) \cdot \text{Cov}_{\pi_{\theta_k}}(z_k(s, a'), \delta_{a', a^*}) \right] \\
&\geq \eta \cdot \left[\sum_{a^* \in \mathcal{A}_2 \cup \mathcal{A}_3} \pi_{\theta_k}(a^*|s) \cdot \text{Cov}_{\pi_{\theta_k}}(z_k(s, a'), \delta_{a', a^*} - \pi_{\theta_k}(a'|s)) \cdot (u - \mathbb{E}_{\pi_{\theta_k}}[z_k(s, a')]) \right] \\
&= \eta \cdot (u - \mathbb{E}_{\pi_{\theta_k}}[z_k(s, a')]) \cdot \left[\sum_{a^* \in \mathcal{A}_2 \cup \mathcal{A}_3} \pi_{\theta_k}(a^*|s) \cdot \text{Cov}_{\pi_{\theta_k}}(z_k(s, a'), \delta_{a', a^*} - \pi_{\theta_k}(a'|s)) \right] \\
&\geq 0
\end{aligned}$$

□